

# RSC Advances



This is an *Accepted Manuscript*, which has been through the Royal Society of Chemistry peer review process and has been accepted for publication.

*Accepted Manuscripts* are published online shortly after acceptance, before technical editing, formatting and proof reading. Using this free service, authors can make their results available to the community, in citable form, before we publish the edited article. This *Accepted Manuscript* will be replaced by the edited, formatted and paginated article as soon as this is available.

You can find more information about *Accepted Manuscripts* in the [Information for Authors](#).

Please note that technical editing may introduce minor changes to the text and/or graphics, which may alter content. The journal's standard [Terms & Conditions](#) and the [Ethical guidelines](#) still apply. In no event shall the Royal Society of Chemistry be held responsible for any errors or omissions in this *Accepted Manuscript* or any consequences arising from the use of any information it contains.



Journal Name

## ARTICLE

# Effects of acidification time of MWCNTs<sup>†</sup> on carbon dioxide capture of liquid-like MWCNTs organic hybrid materials

Ruilu Yang, Yaping Zheng, \*Peipei Li, Haipeng Bai, Yudeng Wang and Lixin Chen

Received 00th January 20xx,  
Accepted 00th January 20xx

DOI: 10.1039/x0xx00000x

www.rsc.org/

In this paper, liquid-like MWCNTs nanoparticles organic hybrid materials (MWCNTs-NOHMs) without solvent at room temperature (25°C) were prepared by employing MWCNTs with different acidification time as core, KH560 as corona and M2070 as canopy. The acidification time of MWCNTs on CO<sub>2</sub> capture capacity of MWCNTs-NOHMs were investigated. The number of amine groups on the surface of MWCNTs-NOHMs increased with the prolongation of acidification time. The CO<sub>2</sub> capture capacity of MWCNTs-NOHMs decreased with extend of acidification time of MWCNTs. This is owe to the superior fluidity, poorer viscosity of shorter acid MWCNTs-NOHM. It provided larger molecule interval and weaker intermolecular forces and made it easier for CO<sub>2</sub> to charge into the potential space. CO<sub>2</sub> can react with amine groups. However, because of the low fluidity and the high viscosity of longer acid MWCNTs-NOHM, its physisorption was unsatisfactory. Chemisorption was also influenced via reducing the contact between CO<sub>2</sub> and reactive groups. The regeneration capacity and adsorption stability of MWCNTs-NOHMs are great, rendering them very potential materials in CO<sub>2</sub> adsorption.

## Introduction

According to the report of the UN Intergovernmental Panel on Climate Change (IPCC), the content of CO<sub>2</sub> is relatively stable until the 18th century. However, rising velocity has increased dramatically since the mid-20th century. It is estimated that CO<sub>2</sub> concentration in the atmosphere will increase doubled than before industrialization in 21 century.<sup>1-3</sup> CO<sub>2</sub> is the main greenhouse gas. It is very significant and demanding to pay immediate attention to the capture and storage of CO<sub>2</sub>.

Alkanolamine is considered as mainly common chemical adsorption material.<sup>4-10</sup> It has high capture capacity, but its adsorption performance can not meet the actual demand. This is because of the corrosion on the reactor, the loss of alkanolamine during reaction due to its high volatility, the high cost of regeneration. Therefore, it is imperative to research the new adsorbent material.<sup>11-16</sup> Organic/inorganic nanocomposite system with both performance of nanoparticles and polymers, has potential applications in material aspects of CO<sub>2</sub> capture.

The liquid-like NOHMs were prepared by ionic<sup>17-19</sup> or covalent bonds<sup>20</sup>. The inorganic nanoparticles were grafted with oligomers. Compared with alkanolamine, there are several advantages of liquid-like nanoparticles organic hybrid materials.<sup>21-27</sup> For instance, noncorrosiveness, zero vapour

pressure, fluidity and structural controllability. As a result of structural controllability, the groups, which can capture CO<sub>2</sub> like amine oligomer, were grafted on the surface of nanoparticles.

Several works<sup>28, 29</sup> have been reported in the field of liquid-like NOHMs for capturing CO<sub>2</sub>. Kun-Yi Andrew Lin and co-workers researched about effects of bonding types and functional groups of liquid-like NOHMs on CO<sub>2</sub> capture, as well as the effect of other gas like SO<sub>2</sub> on CO<sub>2</sub> capture. They found that the capture capacity of liquid-like NOHMs synthesized by covalent bonds was superior. SO<sub>2</sub> changed the CO<sub>2</sub> capture behaviours in liquid-like materials. However, the effect of nanoparticles on CO<sub>2</sub> capture was not mentioned.

Previous studies<sup>11, 30</sup> showed that amine-modified MWCNTs had a certain CO<sub>2</sub> capture capacity and recyclability. This is because MWCNTs have a hollow structure. However, the modified MWCNTs remained solid state at room temperature and aggregated easily. This led to reduction in the contact surface of MWCNTs with CO<sub>2</sub>. Therefore, the CO<sub>2</sub> capture capacity was reduced. Our team had reported the effect of canopy structures on CO<sub>2</sub> capture capacity of MWCNTs-NOHM employing modified MWCNTs as core.<sup>31, 32</sup> The aggregate problem of MWCNTs was solved. At the same time the MWCNTs-NOHM may have a stronger effect in terms of CO<sub>2</sub> capture capacity. The core MWCNT itself had physical capture capacity while the amine groups had chemical capture capacity. The entropy effect also played a role in CO<sub>2</sub> capture capacity.

As core in the MWCNTs-NOHM, acidification of MWCNTs is necessary. The size of cores and surface properties of

School of Nature and Applied Science, Northwestern Polytechnical University, Xi'an 710129, PR China. E-mail: zhengyp@nwpu.edu.cn; Fax: +86-29-88431688

<sup>†</sup> Abbreviations: MWCNTs, multi-walled carbon nanotubes.

MWCNTs will be changed after acidification. The group content on the surface of acid MWCNTs affect the percentage of corona and canopy in the MWCNTs-NOHM and the content of amine groups, which affects the CO<sub>2</sub> capture capacity of MWCNTs-NOHM. In addition, the content of organic chains affect the potential capture space and the active sites of MWCNTs-NOHM. It also greatly affects the CO<sub>2</sub> capture capacity of MWCNTs-NOHM.

In this paper, liquid-like MWCNTs-NOHM with different acidification time of MWCNTs acted as core had been synthesized. The effect of different size and performance of MWCNTs on CO<sub>2</sub> capture capacity had been studied.

## Experimental

### Materials and synthetic procedures

MWCNTs of 20–30 nm diameter and 5–15 μm length were provided by Chengdu organic chemicals Co., Ltd. (3-Glycidyloxypropyl) trimethoxysilane (KH560, 98 wt.%) was from Chengdu aikeda chemicals Co., Ltd. Polyetheramine-M2070 (Mw ~ 2000) was used as polymeric canopy in this study and obtained from Dalian lianhao Co., Ltd. Other analytical grade chemicals were H<sub>2</sub>SO<sub>4</sub>, HNO<sub>3</sub> and methanol.

MWCNTs were modified with mixed acids (H<sub>2</sub>SO<sub>4</sub>/HNO<sub>3</sub>, volume ratio 3:1) at 70°C. The acidification times were 3h, 5h and 7h, respectively. The long organic chains grafted on the surface of MWCNTs as solvent in NOHMs. If the acidification time is not long enough, the –OH and –COOH groups on the surface of MWCNTs are insufficient, leading the number of grafted long organic chains decreased. Thus the NOHMs can not flow like liquid without solvent. Our team had synthesized many MWCNTs-NOHMs with different acidification time of MWCNTs. We found that 3h is the limit of shortest acidification time. For remove residual acid, the products were washed with the deionized water and dried at 70 °C for 24h. Then 5 mmolKH560 was added to the diluted solution of Polyetheramine-M2070 (15wt.%, diluted with methanol and deionized water) dropwise. The molar ratio of KH560 and M2070 was 1 to 1. The mixed solution was stirred for 12h at 45°C. Next, 0.5 g acid MWCNTs were mixed with methanol through the ultrasound dispersion for 30mins, and then added to the mixed solution. The mixture was reacted at 25°C for 5h under mechanicalstirring to ensure complete reaction. The excess M2070 was removed in the dialysis tubing (3500 MWCO, Xi'an luosenbo biotech Co., Ltd) for 12h. At last, the liquid-like MWCNTs-NOHMs were obtained after dried at 35 °C in vacuum oven to remove methanol solvent.

In this study, three specific liquid-like MWCNTs-NOHMs were prepared and named as MWCNTs-NOHM-3h, MWCNTs-NOHM-5h and MWCNTs-NOHM-7h, respectively. It denoted the acidification time of MWCNTs in the liquid-like MWCNTs-NOHMs.

### Characterization

Thermo gravimetric analysis (TGA) measurements were taken under N<sub>2</sub> flowing with heating rate of 10°C /min from 25°C to 600°C by using TGA Q50 TA instrument. A Brookfield R/S plus Rotational Rheometer was used to measure the viscosity of NOHMs with shearing rate of 50s<sup>-1</sup> for 5mins at 25°C. The temperature was stabilized by using a TC-650 constant temperature water bath. Fourier Transform infrared spectra (FTIR) were shown by a WQF-310 FTIR spectrometer and ranged from 400–4000 cm<sup>-1</sup> at room temperature. The samples were measured with KBr pellet. Transmission electron microscope (TEM) images of acid MWCNTs and MWCNTs-NOHM were taken to study the internal morphology of samples. A JEM-2100 instrument was used at an accelerating voltage of 100 kV after a few drops of sample/ethanol solution were placed on a copper grid and dried. X-ray Photoelectron Spectroscopy (XPS, Kratos Axis Ultra DLD) was used to measure the contents of elements and groups of samples. The curves were obtained after a few samples were placed on a conductive blanket. The wide scan ranged from 0eV to 760eV.

Capture CO<sub>2</sub> measurements were tested with a home-made capture instrument<sup>28</sup> (Figure.1). The instrument was made up with a CO<sub>2</sub> cylinder, a pressure transducer (Chengdu lankehedun automation equipment Co., Ltd, CX-206), a press chamber of 30mL volume(recorded as V), an electronic analytical balance (Shanghai yoko instrument Co., Ltd, FA-2004B), a vacuum pump (Wenling suli electromechanical Co., Ltd, 2XZ-4), a few high pressure stainless steel hoses and ball valves. To begin with, the weight of sample was measured by an electronic analytical balance and the reading was recorded as m (g). Next, the MWCNTs-NOHM was put into the press chamber. Before each capture test, any air or gas in the press chamber was removed by vacuum pump. Then CO<sub>2</sub> was introduced into the press chamber. The reading of the pressure transducer was recorded as P1 (MPa) simultaneously. After 30mins, the reading of the pressure transducer was recorded as P2 (MPa). P1 and P2 are both CO<sub>2</sub> pressure. The capture capacity C (mmol/g<sup>-1</sup>) was calculated by equation 1 as follows:

$$C = V(P1 - P2) \times 10^3 / mRT \quad (1)$$

Where R is 8.314(Pa. m<sup>3</sup>/mol.K) and T is 298K.

The desorption process lasted for 10 mins by the vacuum pump. Physisorption was removed and chemisorption remained in this process. Firstly, the sample was exposed to the vacuum environment for 10 mins in case of any gas. Then the initial mass of material was tested by an electronic analytical balance (XS104, METTLER TOLEDO) and was recorded as m (g). After sorption CO<sub>2</sub> for 30 mins and desorption for 10 mins, the mass of material was recorded as m1 (g). Thus the CO<sub>2</sub> chemisorption of material Cc (mmol/g-1) was obtained by equation 2 as follows:

$$C_c = (m1 - m) \times 10^3 / 44m1(2)$$

Then the CO<sub>2</sub> physisorption of material Cp (mmol/g-1) could be calculated to be C-Cc. Furthermore, the sorption-desorption cycle was run 10 times to investigate the regeneration of materials.

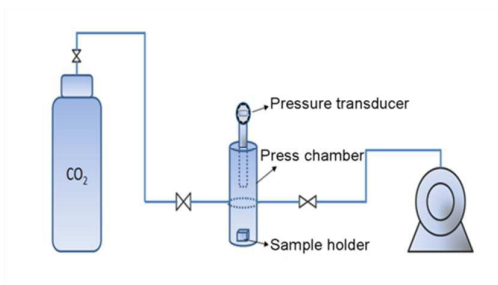


Figure 1. The sketch map of home-made CO<sub>2</sub> capture instrument.

## Results and discussion

### Characterization of MWCNTs-NOHMs

Figure 2 shows the reaction mechanism of acid MWCNTs with KH560 and M2070. The photo in Figure 2 is MWCNTs-NOHM-3h and shows black viscous flow state at room temperature. This is attributed to the layer of organics, which is consisted of long chains of KH560 and M2070. As a result of this organic layer, the MWCNTs-NOHMs possess both lipophilic and hydrophilic. The three samples were placed on glass slide inclined 30° for 10 mins at room temperature as photographed in Figure 3. From these images we can see that the three samples flowed in the absence of solvents on glass slide and remained black viscous flowing tracks. The track of MWCNTs-NOHM-3h is the longest which shows the best fluidity. MWCNTs-NOHM-5h is the secondary one.

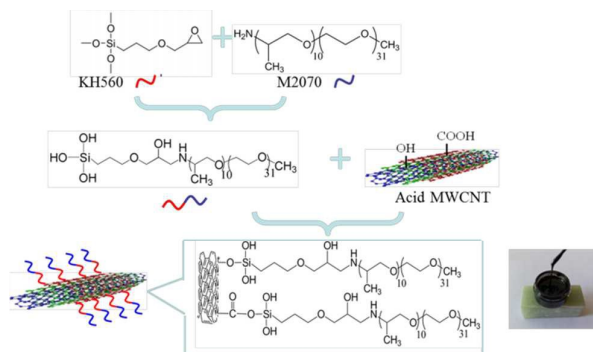


Figure 2. the reaction mechanism and structure of acid MWCNTs with KH560 and M2070

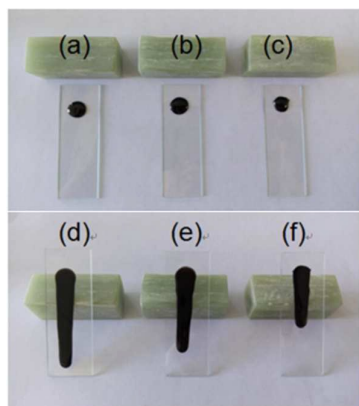


Figure 3. Fluidity photos of MWCNTs-NOHMs inclined 30° for 10 mins at room temperature, (a), (b) and (c) initial state of MWCNTs-NOHM-3h, 5h and 7h. (d), (e) and (f) final state of MWCNTs-NOHM-3h, 5h and 7h after 10 mins

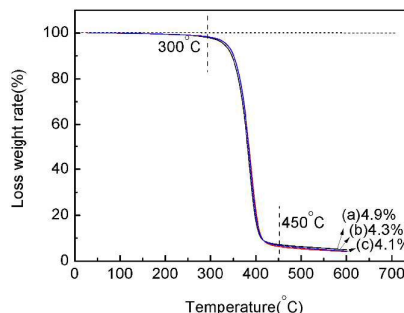


Figure 4. TGA curves of (a) MWCNTs-NOHM-3h, (b) MWCNTs-NOHM-5h, (c) MWCNTs-NOHM-7h.

The TGA curves of NOHMs are shown in Figure 4. The loss weight of NOHMs is few below 300 °C. It reveals that the NOHMs without solvent still show liquid-like state at room temperature, owing to the flexible long chains of polyetheramine as canopy. Thereby, the NOHMs are stable as CO<sub>2</sub> capture sorbents. Moreover, corona and canopy are decomposed above 300 °C. Nanoparticles are left over above 450 °C. It indicates that the contents of core in MWCNTs-NOHM-3h, 5h and 7h are up to 4.9 wt.%, 4.3 wt.% and 4.1 wt.%, respectively. Then the content of KH-560 and M-2070 in MWCNTs-NOHM-3h, 5h and 7h are 95.1 wt.%, 95.7 wt.% and 95.9 wt.%, respectively. The dense surface coverage recorded as  $n$  is used to represent the number of carbon atoms of per organic chain (KH560 and M2070) grafted on MWCNTs. It is calculated by formula (5).

$$n = \frac{\omega_c}{M_c} \bigg/ \frac{\omega_o}{M_o} \quad (5)$$

Where  $\omega_c$  and  $\omega_o$  represent the weight fraction of carbon atoms and organism in the system.  $M_c$  and  $M_o$  are the mole mass of carbon atoms and organism, and are up to 12 g·mol<sup>-1</sup> and 2236 g·mol<sup>-1</sup>, respectively. The dense surface coverage of MWCNTs-NOHMs-3h, 5h and 7h are 9.6, 8.3 and 7.9, respectively. It means that every 10 organic chains share 96 carbon atoms in MWCNTs-NOHMs-3h, 83 carbon atoms in MWCNTs-NOHMs-5h and 79 carbon atoms in MWCNTs-NOHMs-7h. It indicates that longer acidification time of MWCNTs make more organic chains, which provide amine groups in MWCNTs-NOHM.

To compare the viscosity of NOHMs, the viscosity curves of MWCNTs-NOHMs at 25 °C are shown in Figure 5. The MWCNTs-NOHM-7h presents the highest viscosity of NOHMs, reaching to 11.5 Pa·s. Besides, the viscosity of MWCNTs-NOHM-3h is the lowest, only 9.5 Pa·s. This result is consistent with the photos which are shown in Figure 3. Furthermore, the results of TGA indicate that the smaller value of dense surface coverage  $n$ , the more organic chains in MWCNTs-NOHMs. This leads to more friction and less space between the chains, and limiting the molecular chains movement. As a result, the viscosity of MWCNTs-

NOHMs is increased. So the dense surface coverage  $n$  affects the viscosity of MWCNTs-NOHMs. Smaller value of  $n$  makes larger viscosity of MWCNTs-NOHMs.

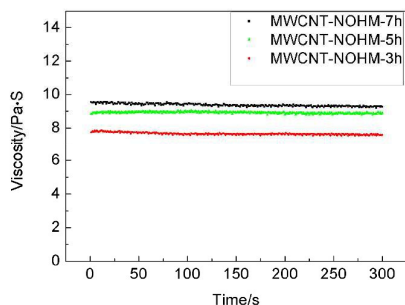


Figure 5. The viscosity curves of MWCNTs-NOHMs at 25 °C

The FTIR spectra of MWCNTs-NOHMs are illustrated in Figure 6. The spectra of MWCNTs with different acidification time are also included for comparison. When the KH560 is grafted onto the surface of MWCNTs via dehydration-condensation reaction, new absorption band  $709\text{ cm}^{-1}$  appears, which is assigned to C-O-Si stretching vibrations in the curves (a), (b) and (c). In these curves, band at  $1290\text{ cm}^{-1}$  correspond to the secondary amine group -NH- vibrations. This is due to the reaction between epoxy groups of KH560 and -NH<sub>2</sub> of M2070. As expected, the MWCNTs-NOHMs show peaks characteristic of both the KH560 and M2070. The new peaks at  $1189\text{ cm}^{-1}$ ,  $1120\text{ cm}^{-1}$  and  $1471\text{ cm}^{-1}$  are assigned to the absorption peak of aliphatic amine, vibrations of ether bond -O- and in-plane bending vibration peak of C-H, respectively. The result of FTIR spectra demonstrates that the MWCNTs-NOHMs were prepared successfully. In order to further demonstrate that the reaction has occurred, FTIR spectra of pristine M2070, intermediate product KH560+M2070 and MWCNTs-NOHMs from  $2800\text{--}4000\text{ cm}^{-1}$  are shown in Figure 7. Two characteristic absorption peaks of -NH<sub>2</sub> near  $3290\text{ cm}^{-1}$  and  $3360\text{ cm}^{-1}$  are observed in the spectra of pristine M2070. The disappearance of these two absorption peaks in the intermediate product KH560+M2070 indicate that KH560 has been successfully grafted to M2070. Furthermore, the -NH<sub>2</sub> absorption peaks are not observed in MWCNTs-NOHMs. To combine with the absorption peaks in Figure 6 of MWCNTs-NOHMs, the organic layer is grafted to MWCNTs successfully.

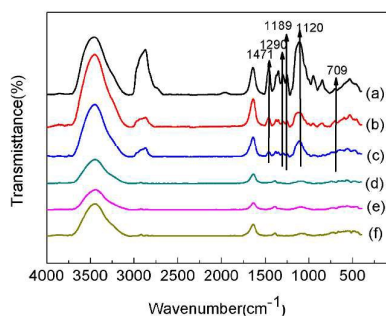


Figure 6. FTIR spectra of acid MWCNTs and MWCNTs-NOHMs, (a) MWCNTs-NOHM-3h, (b) MWCNTs-NOHM-5h, (c) MWCNTs-NOHM-7h, (d) MWCNTs-3h, (e) MWCNTs-5h, (f) MWCNTs-7h

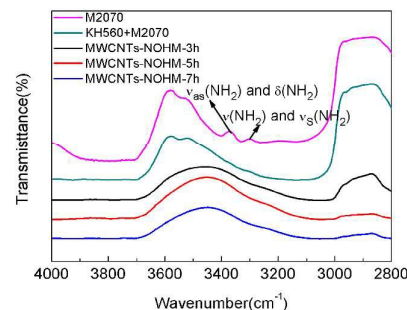


Figure 7. FTIR spectra of pristine M2070, intermediate product KH560+M2070 and MWCNTs-NOHMs.

The TEM images (Figure 8(a), (b) and (c)) show different acidification time of acid MWCNTs. In these images, the length of acid MWCNTs gradually diminished as acidification time become longer. In image (b), the outer wall of acid MWCNTs is decomposed by acids and appears slub. The phenomenon is more obvious in image (c). It is demonstrated that the size of MWCNTs change with the acidification time. The images show that the acid MWCNTs were wrapped with a layer of organics (Figure 8(d), (e), (f)) and reveal that the MWCNTs-NOHM were synthesized successfully, which is consistent with the result of FTIR.

The XPS curves of pristine MWCNTs and acid MWCNTs are shown in Figure.S1, Figure.9 and Figure.S2. The C1s photoelectron is in  $284\text{ eV}$  and the O1s photoelectron is in  $532\text{ eV}$ . The wide scan curves of pristine MWCNTs and acid MWCNTs are shown in Figure.S1 (a) and



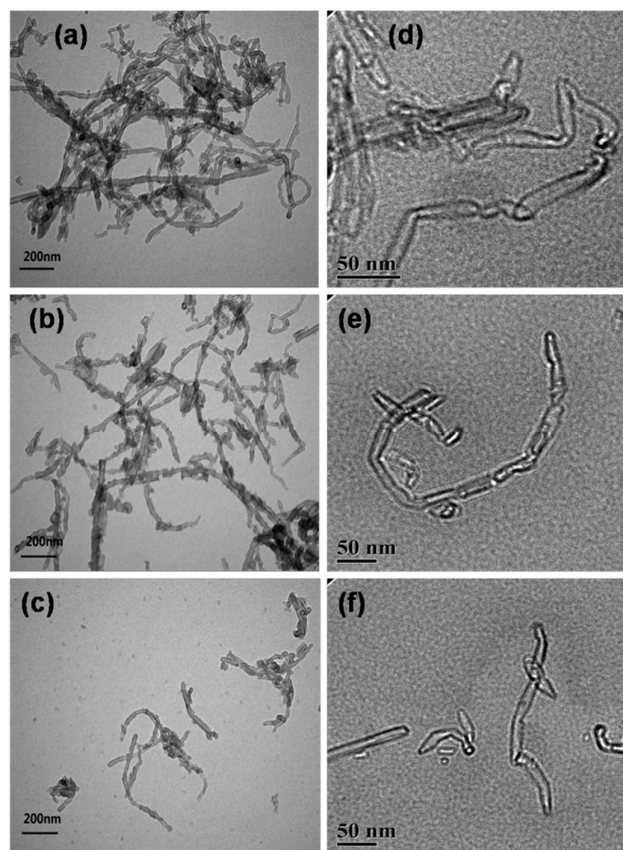


Figure.8 TEM images of different acidification times of acid MWCNTs and MWCNTs-NOHMs. (a) MWCNTs-3h, (b) MWCNTs-5h, (c) MWCNTs-7h, (d) MWCNTs-NOHM-3h, (e) MWCNTs-NOHM-5h, (f) MWCNTs-NOHM-7h.

Figure.S2 (a)-(c), which demonstrate that the oxygen-containing groups are generated on the surface of MWCNTs after acidification. It can be seen clearly that the content of oxygen-containing groups increased with the acidification time of MWCNTs increasing. This is owing to the breaking of MWCNTs during acidification. Thereby a large number of oxygen-containing groups like -C-O, C=O and O-C=O are generated.

After a Gaussian curve fitting process, the peak of C1s is divided into four peaks as follows: C-C bond energy in  $284.5 \pm 0.5$  eV, -C-O- bond energy in  $286.6 \pm 0.5$  eV, -C=O bond energy in  $287.8 \pm 0.5$  eV, O-C=O bond energy in  $288.9 \pm 0.5$  eV. All of these narrow scan curves are illustrated in Figure.S1 (b) and Figure.9 (a)-(c). After acidification, the content of -COOH increased. Besides, the content of -COOH groups increased as acidification time of acid MWCNTs become longer. From XPS curves of acid MWCNTs, the mass fraction of grafted groups -COOH ( $\omega_{\text{COOH}}$ ) and -OH ( $\omega_{\text{OH}}$ ) are gained. They are calculated by the formula (3) and (4) as follow:

$$\omega_{\text{COOH}} = \frac{\omega_{\text{C1S}} \times \omega_{\text{COOH}}^{\text{C1S}}}{M_{\text{C}}} \times M_{\text{COOH}} \times 100\% \quad (3)$$

$$\omega_{\text{OH}} = \frac{\omega_{\text{C1S}} \times \omega_{\text{COH}}^{\text{C1S}}}{M_{\text{C}}} \times M_{\text{OH}} \times 100\% \quad (4)$$

Where  $\omega_{\text{C1S}}$  presents the weight fraction of C1s in wide scan XPS curves. The mass fraction of C1s in narrow scan XPS curves based on -COOH and -COH are recorded as  $\omega_{\text{COOH}}^{\text{C1S}}$  and  $\omega_{\text{COH}}^{\text{C1S}}$  respectively.  $M_{\text{C}}$ ,  $M_{\text{COOH}}$  and  $M_{\text{OH}}$  are molar mass. They are  $12 \text{ g} \cdot \text{mol}^{-1}$ ,  $45 \text{ g} \cdot \text{mol}^{-1}$  and  $17 \text{ g} \cdot \text{mol}^{-1}$ , respectively. Therefore, according to formula (3) and (4), the  $\omega_{\text{COOH}}$  in NOHM-3h, 5h and 7h are 13.16 wt.%, 24.9 wt.% and 27.76 wt.%, respectively. Moreover, the  $\omega_{\text{OH}}$  in NOHM-3h, 5h and 7h are 33.01 wt.%, 27.87 wt.% and 27.85 wt.%, respectively, because oxidation of -OH yields -COOH. From these evidences we can see that longer acidification time of MWCNTs causing larger total mass fraction of grafted groups in acid MWCNTs.

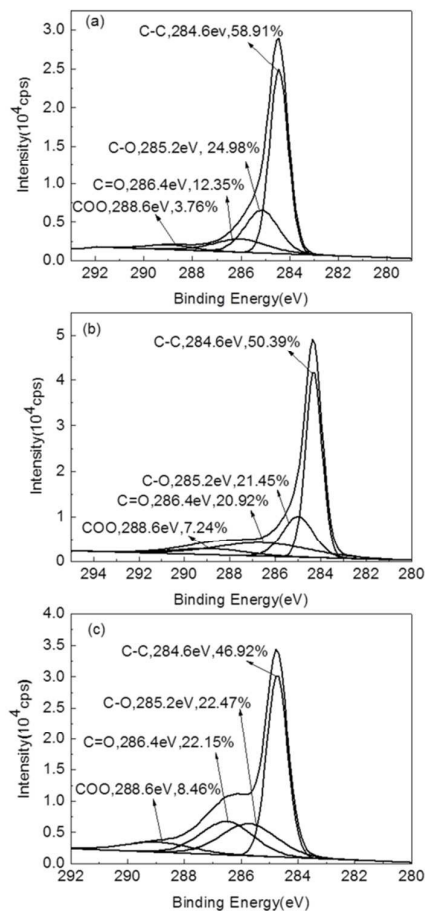


Figure.9. XPS curves of C1s narrow scan of acid MWCNTs, (a) MWCNTs-3h, (b) MWCNTs-5h, (c) MWCNTs-7h

The polymeric corona KH560 can react with -C-OH group and O-C=O group of acid MWCNTs. Therefore, the surface of acid MWCNTs with 7h acidification is grafted with more organic chains and obtains more amine groups from M2070.

The peaks at 400 eV and 100 eV correspond to N1s and Si2p of MWCNTs-NOHM in Figure.S3 (a)-(c). The contents of these two elements are both risen with the increasing of acidification time. It also certificates that MWCNTs-NOHM-7h get more amine groups. The Gaussian curves of C1s of MWCNTs-NOHM

are shown in Figure.10 (a)-(c). The covalent bonds C-N and C-Si formed owing to the reaction shown in Figure.2.

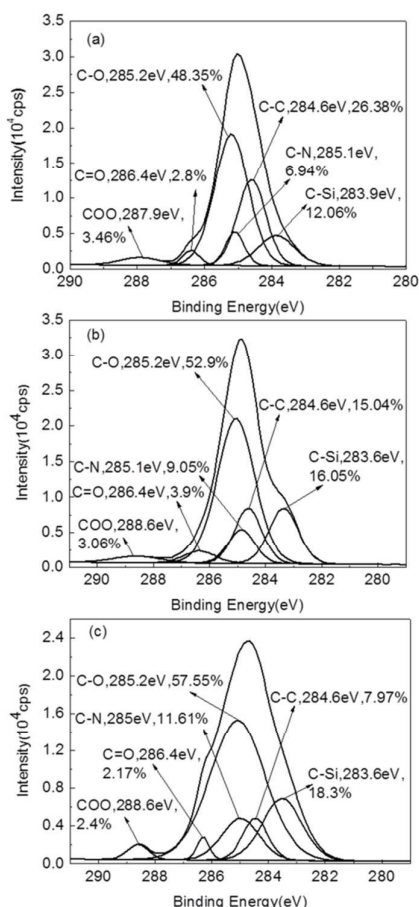


Figure.10. XPS curves of C1s narrow scan of MWCNTs-NOHMs, (a) MWCNTs-NOHM-3h, (b) MWCNTs-NOHM-5h, (c) MWCNTs-NOHM-7h

#### Study of CO<sub>2</sub> capture capacity of MWCNTs-NOHMs

Ping Qu<sup>31</sup> and Peipei Li<sup>32</sup> have reported the effect of canopy structures on CO<sub>2</sub> capture capacity of MWCNTs-NOHM. Not only does the canopy structure, but also the core structure has an important influence on CO<sub>2</sub> capture. In this paper, the effects of different acidification time of MWCNTs as core on CO<sub>2</sub> capture capacity have been studied. CO<sub>2</sub> capture capacity under different CO<sub>2</sub> pressure at room temperature is demonstrated in Figure.11.

It can be seen that the pristine MWCNTs shows lowest adsorption of CO<sub>2</sub> under all CO<sub>2</sub> pressure may be due to its none reactive groups with CO<sub>2</sub> and the hollow structure of MWCNTs can only provide physisorption. The pristine canopy M2070 presents liquid state at room temperature and its CO<sub>2</sub> capture capacity is better than pristine MWCNTs. This is because the primary amine groups of M2070 provide chemisorptions. Besides, physisorption is also exists for M2070.

As shown in Figure.11, the CO<sub>2</sub> capture capacity of three MWCNTs-NOHMs are increased with increasing capture

pressure and are all much better than pristine MWCNTs and canopy M2070, and even exceed the summation of them under the same CO<sub>2</sub> pressure. As a result of it, The MWCNTs-NOHMs are proved to be very potential materials in CO<sub>2</sub> adsorption. They are more significant than the previous work reported by K.Y. Andrew Lin and A.H. Alissa Park.<sup>20</sup> They found that CO<sub>2</sub> capture capacity of tPE was slightly better than that of NOHM-I-tPE. It is owing to a portion of amine group was consumed during the synthesis of NOHM-I-tPE. The CO<sub>2</sub> capture capacity of MWCNTs-NOHM

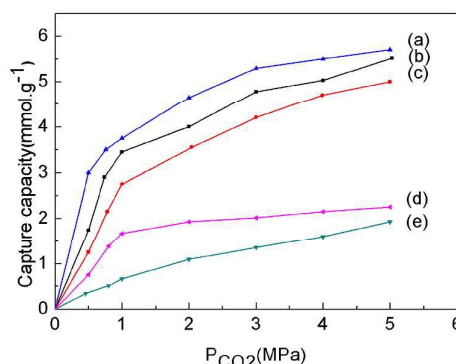


Figure.11. CO<sub>2</sub> capture capacity of (a) MWCNTs-NOHM-3h, (b) MWCNTs-NOHM-5h, (c) MWCNTs-NOHM-7h, (d) M2070, (e) pure MWCNTs under 0-5 MPa of CO<sub>2</sub> at room temperature.

It is obvious that the CO<sub>2</sub> capture capacity of MWCNTs-NOHMs become well with the shorter acidification time under the same CO<sub>2</sub> pressure. It seems that MWCNTs-NOHM-7h with the most groups has superior CO<sub>2</sub> capture capacity. However, the interesting result is that the CO<sub>2</sub> capture capacity of MWCNTs-NOHM-7h is the worst among the three MWCNTs-NOHMs. This is may be due to the lower fluidity and higher viscosity of MWCNTs-NOHM-7h, reducing the number of amine groups which can react with CO<sub>2</sub>. For further investigation of effects on acidification time of MWCNTs on CO<sub>2</sub> capture, the chemisorption and physisorption of MWCNTs-NOHMs under different CO<sub>2</sub> pressure at room temperature are shown in Figure.12.

Figure.12 (a) is the chemisorption of pristine MWCNTs, M2070 and three kinds of MWCNTs-NOHMs. It is easily found that the pristine MWCNTs show negligible chemisorption. Its adsorption behaviour is all shown in Figure.12. (b), which shows the physisorption of samples. As shown in Figure.12, the physisorption of pristine M2070 is the minimum. However, its chemisorption is the maximal due to its relatively higher content of primary amine groups in unit mass of M2070. In addition, for these three MWCNTs-NOHMs, the chemisorption of MWCNTs-NOHM-3h is the lowest owing to its low content of secondary amine groups with shorter acidification time of MWCNTs. This result is based on the result of XPS data shown in Figure.10. As the result of XPS test, the content of secondary amine groups of MWCNTs-NOHM-7h is higher than that of MWCNTs-NOHM-5h, but the Figure.12 (a) shows the contrary

Journal Name

LE

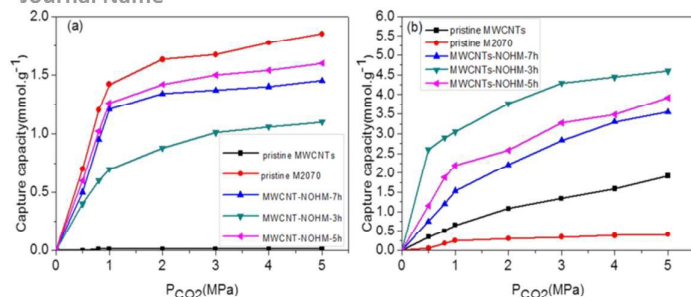


Figure.12 (a) chemisorption  $\text{CO}_2$  capture capacity of MWCNTs-NOHMs, (b) physisorption  $\text{CO}_2$  capture capacity of MWCNTs-NOHMs under 0-5MPa of  $\text{CO}_2$  at room temperature.

result. The chemisorption of MWCNTs-NOHM-7h is little lower than MWCNTs-NOHM-5h. It is because some secondary amine groups are isolated from  $\text{CO}_2$  due to the lowest fluidity and the highest viscosity of MWCNTs-NOHM-7h. They reduce the contact between  $\text{CO}_2$  and reactive groups. Furthermore, It is clearly seen that physisorption of MWCNTs-NOHMs become lower with the prolongation of acidification time. The physisorption of MWCNTs-NOHMs are mainly based on two ways, namely, hollow structure of MWCNTs and potential space between long chains of corona and canopy. The shorter acidification time MWCNTs-NOHM-3h with superior fluidity and poorer viscosity provide larger molecule interval and weaker intermolecular forces and made it easier for  $\text{CO}_2$  to charge into the potential space. Therefore, the  $\text{CO}_2$  capture capacity of MWCNTs-NOHM-3h is the best integratedly.

Haipeng Bai<sup>33</sup> reported the NOHM based on POSS, K.Y. Andrew Lin<sup>29</sup> reported the NOHM based on  $\text{SiO}_2$  and George Em. Romanos<sup>34</sup> reported the silica nanoparticles encapsulating amine functionalized Ionic Liquids. The  $\text{CO}_2$  capture capacity of POSS-NOHM,  $\text{SiO}_2$ -NOHM and Si-IL is relatively lower than MWCNTs-NOHMs we reported because POSS and  $\text{SiO}_2$  nanoparticles have no hollow structure like MWCNTs. The best  $\text{CO}_2$  capture capacities of each material are shown and compared in Table.1.

Table.1.  $\text{CO}_2$  capture capacities of different adsorbents

adsorbents	MWCNTs-NOHM	POSS-NOHM	$\text{SiO}_2$ -NOHM	$\text{SiO}_2$ -IL
$\text{CO}_2$ capture capacities/ $\text{mmol.g}^{-1}$	5.5	3.8	3.7	3.4

For further study, Figure.13 shows the  $\text{CO}_2$  capture data of MWCNTs-NOHMs via 10 times sorption-desorption cycles under 2MPa  $\text{CO}_2$  pressure at room temperature. It indicates clearly that there are no efficiency loss and degradation of MWCNTs-NOHMs even via 10 times sorption-desorption cycles. The regeneration capacity and adsorption stability of MWCNTs-NOHMs are great.

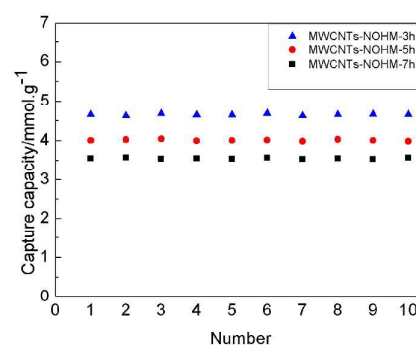


Figure.13.  $\text{CO}_2$  capture capacity MWCNTs-NOHMs via 10 sorption-desorption cycles under 2MPa  $\text{CO}_2$  pressure at room temperature

site 1  $\text{CO}_2 + \text{R}_1\text{R}_2\text{NH} \rightleftharpoons \text{R}_1\text{R}_2\text{N}^+\text{HCO}_2^-$  Chemisorption  
 site 2 Hollow structure of MWCNTs } Physisorption  
 site 3 Potential space between long organic chains }

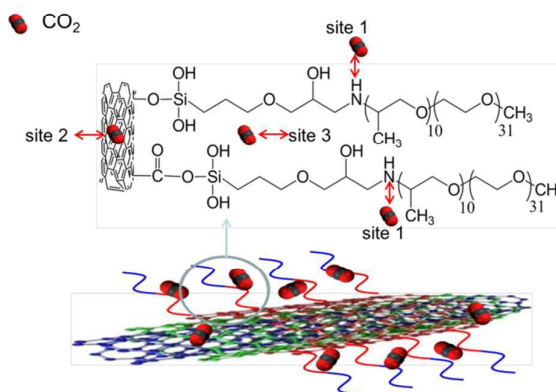


Figure.14.  $\text{CO}_2$  capture mechanism of MWCNTs-NOHM.

Finally, on the basis of the above results, the  $\text{CO}_2$  capture mechanism of MWCNTs-NOHM is illustrated in Figure.14. It can be easily found that more content of  $-\text{NH}-$  make higher chemisorption. On the contrary, higher viscosity is disadvantageous to both chemisorption and physisorption because it not only reduces the contact between  $\text{CO}_2$  and  $-\text{NH}-$ , but also provides larger molecule interval and weaker intermolecular forces, which make it easier for  $\text{CO}_2$  to charge into the potential space. Besides, longer acidification time of MWCNTs make more content of  $-\text{NH}-$  and higher viscosity of NOHMs. After all, longer acidification time of MWCNTs leads to lower  $\text{CO}_2$  adsorption.

## Conclusions

Liquid-like MWCNTs organic hybrid materials (MWCNTs-NOHMs) were prepared by employing MWCNTs different acidification time as core, KH560 as corona and M2070 as canopy. It is found that longer acidification time of MWCNTs make more content of amine groups in MWCNTs-NOHMs. In the meantime, the viscosity of MWCNTs-NOHMs increased with longer acidification time. From the test of  $\text{CO}_2$  capture capacity, it is concluded that more content of  $-\text{NH}-$  make



higher chemisorption. On the contrary, higher viscosity is disadvantageous to both chemisorption and physisorption because it not only reduces the contact between CO<sub>2</sub> and -NH-, but also provides larger molecule interval and weaker intermolecular forces, which make it easier for CO<sub>2</sub> to charge into the potential space. Therefore, longer acidification time of MWCNTs causing worse CO<sub>2</sub> capture capacity of MWCNTs-NOHMs. The regeneration capacity and adsorption stability of MWCNTs-NOHMs are great. They are very potential materials in CO<sub>2</sub> adsorption.

## Acknowledgements

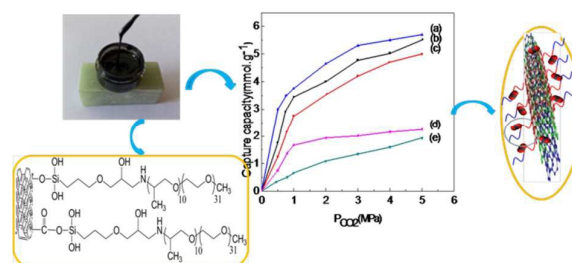
This work is supported financially by the National Natural Science Foundation (51373137) and the fund of the Innovation Base of Graduate Students of NPU.

## Notes and references

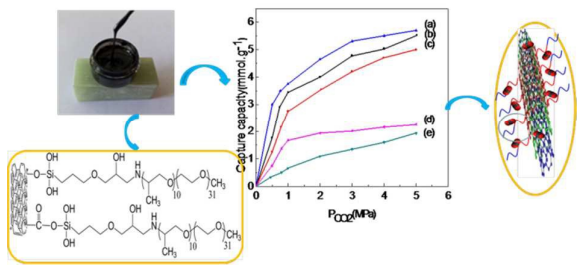
- Intergovernmental Panel in Climate Change (IPCC). Climate Change 2007: The Physical Science Basis, R. UK: Cambridge University Press. 2007.
- Intergovernmental Panel in Climate Change (IPCC). IPCC Special Report on Carbon Dioxide Capture and Storage, R. UK: Cambridge University Press. 2005.
- P. N. Pearson and M. R. Palmer, *Nature*, 2000, **406**, 695-9.
- G. Qi, *Energy & Environmental Science*, 2011, **2**, 444-452.
- G. Qi, L. Fu and E.P. Giannelis, *Nature Communications*, 2014, **5**, 5796-5796.
- P. Singh and G. F. Versteeg, *Process Safety & Environmental Protection*, 2008, **5**, 347-359.
- Dubois, L, P. K. Mbasha and D. Thomas, *Chemical Engineering & Technology*, 2010, **3**, 461-467.
- C. H. Yu, *Aerosol & Air Quality Research*, 2012, **5**, 745-769.
- C. Dinca, *Journal of Cleaner Production*, 2016, **112**, 1136-1149.
- K. Osman, D. Ramjugernath and C. Coquelet, *Journal of Chemical & Engineering Data*, 2015, **8**, 2380-2391.
- S. Fengsheng, L. Chungsyng and C. Hung-Shih, *Langmuir the Acs Journal of Surfaces & Colloids*, 2011, **13**, 8090-8098.
- C. Lu, *Energy & Fuels*, 2008, **22**, 3050-3056.
- S. C. Hsu, *Chemical Engineering Science*, 2010, **4**, 1354-1361.
- B. A. Thinsp, *Advanced Functional Materials*, 2005, **8**, 1285-1290.
- S. Denizalt, *RSC Advances*, 2015, **5**, 45454-45458.
- F. W. M. D. Silva, *Adsorption Science & Technology*, 2015, **2**, 223-242.
- K. J. Fricker and A. H. A. Park, *Chemical Engineering Science*, 2013, **2**, 332-341..
- M. L. Jespersen, *Acs Nano*, 2010, **7**, 3735-3742.
- L. Lan, *Journal of Nanoparticle Research*, 2012, **3**, 1-10.
- K. Y. A. Lin and A. H. A. Park, *Environmental Science & Technology*, 2011, **15**, 6633-9.
- J. X. Zhang, *Polymer*, 2009, **13**, 2953-2957.
- A. B. Bourlinos, *Small*, 2006, **10**, 1188-91.
- R. Rodriguez, *Advanced Materials*, 2008, **22**, 4353-4358.
- J. X. Zhang, *Soft Materials*, 2010, **1**, 39-48.
- A. B. Bourlinos, *Advanced Materials*, 2005, **2**, 234-237.
- A. B. Bourlinos, *European Physical Journal E Soft Matter*, 2006, **1**, 109-117.
- C. Petit, *Journal of Chromatography A*, 2011, **1**, 141-151.
- K. Y. A. Lin, C. Petit and A. H. A. Park, *Energy Fuels*, 2013, **8**,

4167-4174.

- Y. Park, *Journal of Chemical & Engineering Data*, 2012, **1**, 40-45.
- A. K. Mishra and S. Ramaprabhu, *Rsc Advances*, 2012, **5**, 1746-1750.
- P. Qu, *Colloid & Polymer Science*, 2015, **6**, 1-12.
- P. P. Li, *Carbon*, 2015, **95**, 408-418.
- H. P. Bai and Y.P. Zheng, *Materials & Design*, 2016, **99**, 145-154.
- G. E. Romanos, *Journal of Physical Chemistry C*, 2014, **42**, 24437-24451.



**The structure and surface properties of MWCNTs as core in NOHM have a significant influence on CO<sub>2</sub> capture**



The structure and surface properties of MWCNTs as core in NOHM have a significant influence on CO<sub>2</sub> capture